

Molecular gas dynamics and AGN/starburst mechanism in a strongly-lensed wet merger: bridging the gap between local ULIRGs and high- z systems

PI: T. K. Daisy Leung

Missing link between mergers/ULIRGs and their high- z analogues Ultraluminous infrared galaxies (ULIRGs: $L_{\text{IR}} \geq 10^{12} L_{\odot}$) have been regarded as analogues of high-redshift (z) starbursts given the similarities in their interstellar medium (ISM; e.g. $L_{\text{IR}}/L'_{\text{CO}}$). As such, detailed studies of ULIRGs are important to gain more detailed insight into the early universe and in studies of galaxy evolution over cosmic time. While mergers are believed to play an important role in giving rise to these dusty galaxies (e.g. Sanders & Mirabel 1996), merger-induced effects on the physical mechanisms and chemistry that drive the starburst (SB) and active galactic nucleus (AGN) activities on small scales are still unclear. Thus characterizing the properties of the molecular gas that fuels star-formation (SF) and AGN is crucial to understand the interplay between AGN and SB and their relation to the ISM properties of galaxies across cosmic time.

While the ISM in local ULIRGs has been studied in great detail, forming a rich inventory of molecular transitions that serves as the template for studying high- z galaxies (e.g. Rangwala et al. 2015), a wide knowledge gap persists between $z=0$ and the epoch when most stars are formed in the universe ($z \sim 2$). Hence, understanding galaxy populations at an epoch when the build-up of stellar mass is steeply rising is critical and we here aim to bridge this gap by testifying correlations and properties found locally out to high redshift by observing the dynamical structure and properties of the ISM of the quadruply lensed galaxy RXJ1131-1231 and its dust-obscured companion at $z_{\text{CO}} \sim 0.65$ (Fig. 1).

Molecular gas in AGN/SB Owing to the high molecular gas fractions in ULIRGs, their extreme SFRs are a natural consequence of either gas is being converted into stars more efficiently and/or their molecular gas content. Fragmentation of giant star-forming clumps and turbulent conditions are also expected from gravitational instability of these gas-rich bodies. In fact, studies of the ISM kinematics at $z=1-2$ find clumps of size scale \sim few kpc (Swinbank et al. 2012a,b). Resolving the gas dynamics on hundred pc scales is therefore an important first step to understanding the mechanisms and physical processes taking place on different scales and how the ISM physical conditions are related to the SB in ULIRGs at this epoch.

While ^{12}CO emission traces the total molecular distribution and dynamics, high-dipole moment molecules such as HCN and HCO^+ are expected to trace the denser, actively star-forming gas. Indeed, a tight correlation between $\text{HCN}(J=1 \rightarrow 0)$ and L_{IR} (proxy for SFR) has been found in nearby galaxies and local giant molecular clouds (GMC; Gao & Solomon 2004, hereafter GS04; Wu et al. 2005), suggesting HCN is a faithful tracer of the star-forming dense gas. However, $\text{HCN}(J=4 \rightarrow 3)$ observations of (U)LIRGs have revealed a wide range of excitation conditions that may render the ground state transition of HCN and HCO^+ poor proxies of the dense gas mass (Papadopoulos 2007, hereafter P07). In this light, higher- J transitions (e.g. $J=4 \rightarrow 3$) have been suggested to be better probes since they trace the much denser gas ($n \gtrsim 10^5 - 10^7 \text{ cm}^{-3}$) that is thought to be the immediate fuel for SF in turbulent GMCs (Shirley et al. 2003; Krumholz & McKee 2005). This has been supported by the linear correlations found in $L_{\text{IR}} - L'_{\text{HCN}(J=4 \rightarrow 3)}$ and $L_{\text{IR}} - L'_{\text{HCO}^+(J=4 \rightarrow 3)}$ (Zhang et al. 2014). Since the ground state lines are redshifted to frequencies beyond the spectral coverage of ALMA at $z > 0.06$, it is also necessary to establish diagnostics using these mid- J lines to study distant galaxies. Additionally, due to the difference in abundances and excitation conditions of HCN and HCO^+ in star-forming versus AGN regions, the line ratio $\text{HCN}(J=4 \rightarrow 3)/\text{HCO}^+(J=4 \rightarrow 3)$ (Imanishi & Nakanishi 2014; García-Burillo et al. 2014; Viti et al. 2014) have been proposed as a diagnostic tool to reveal deeply buried AGNs at the cores of ULIRGs (Izumi et al. 2016; Imanishi et al. 2016).

Prior to ALMA, studies of dense gas were largely limited to the local universe ($z \lesssim 0.1$) with only five detections at $z \gtrsim 0.3$ (e.g. Riechers et al. 2007, 2010; Wagg et al. 2005; Gao et al. 2007). Moreover, none of these spatially resolve the emission, rendering it difficult to draw more detailed conclusions on the dense gas properties of galaxies at high z . Even with ALMA, such studies will remain challenging, but by combining the magnification provided by gravitational lensing with the exceptional spatial resolution and sensitivity of ALMA, studies of dense molecular gas in distant galaxies are now possible, as proposed here.

Science Target RXJ 1131-1231: a demonstrative case at high- z

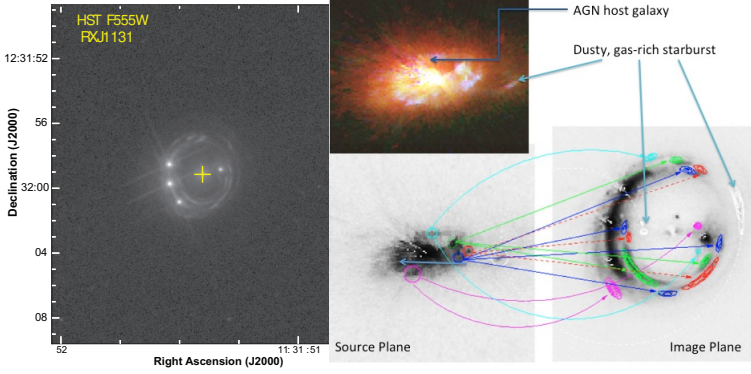


Figure 1: Stellar light distribution in the AGN host galaxy of RXJ 1131-1231 and its reconstructed source plane morphology *Left:* The rest-frame UV emission (tracing recent star formation) is lensed into an almost complete Einstein ring with diameter $\sim 3.8''$. *Right:* Lens modeling of the optical emission identifies complex structures in the host galaxy and an optically faint companion (white; Claeskens et al. 2006), which we have recently confirmed by modeling CO($J=2 \rightarrow 1$) emission detected with NOEMA (Fig. 4; Leung & Riechers, in prep.). We here propose to study the ISM conditions in this AGN-starburst merger with finer detail than otherwise possible with current facilities.

RXJ 1131-1231 is a quadruply imaged AGN with its host galaxy lensed into a partial Einstein ring (Fig. 1). HST observations (rest-frame UV) have revealed distinct emission from recent star formation (lensing arcs) and from the AGN (bright knots) in the background galaxy (Sluse et al. 2003), demonstrating the great potential for probing its ISM conditions in detail. Lens modeling carried out on optical images shows that the AGN resides in a star-forming region of size ~ 1 kpc in its host galaxy, which itself is 7 kpc across, and made it possible to identify seven distinct structures in the source plane (Fig. 1). Remarkably, emission from a spatially offset region (~ 2.4 kpc away from the AGN host galaxy) has been identified and found to be ~ 700 pc in size (Brewer & Lewis 2008), indicating a companion galaxy. We have recently confirmed that both galaxies are at the same redshift by detecting their CO($J=2 \rightarrow 1$) emission and lens-modeling their gas distribution in velocity space (Fig. 4f), and verified that the both are gas-rich (Leung & Riechers, in prep.). Our SED modeling of the dust continuum emission up to $250 \mu\text{m}$ finds $L_{\text{IR}} \sim 6 \times 10^{12} L_{\odot}$ (corrected for lensing). Hence, this target is a gas-rich ULIRG merger at $z \sim 0.7$ caught in the act.

Proposed Observations and Science Goals We here propose to map (1): CO($J=5 \rightarrow 4$) at $0.15''$ resolution (~ 500 pc at $z \sim 0.7$ in the source plane) and (2): HCN($J=4 \rightarrow 3$) and HCO $^+$ ($J=4 \rightarrow 3$) emission and the underlying continuum at $0.7''$ resolution (2.5 kpc in the source plane). The continuum traces the dust emission, providing better constraints on the gas-to-dust ratio, dust temperature(s), dust mass, and its spatial extent (and thus the surface density of the SFR). These quantities are key to investigate how the ISM vary as galaxies evolve across cosmic time. In conjunction with the large set of ancillary data from rest-frame UV to radio wavelength and our recent observations of CO($J=2 \rightarrow 1$) and CO($J=3 \rightarrow 2$), our proposed observations are designed to investigate the gas-rich merger in aspects listed as follows.

Dynamics and kinematics: Our recently obtained CO($J=2 \rightarrow 1$) data shows an asymmetric double-horned line profile (Fig. 4a). Given the 1st moment map observed and the velocity gradient across the source plane in our model (Fig. 4d & 4f), this is indicative of a kinematically ordered galaxy, but its emission has been lensed differentially. Limited by the spatial resolution of this data, it is not possible to infer the true kinematics due to beam smearing. Furthermore, the unusually high velocity dispersion $\gtrsim 400 \text{ km s}^{-1}$ at the central region (Fig. 4e) hints at perturbations from the AGN and/or internal turbulence due to interactions with the companion and/or instability due to the huge gas reservoir. Thus higher-resolution CO($J=5 \rightarrow 4$) imaging, as proposed here, is needed to distinguish between a merger-driven and a turbulent clumpy disk starburst,

The requested resolution ($0.15''$) for CO($J=5 \rightarrow 4$) is critical as it allows us to obtain a detailed dynamical lens model of the system, probing at sub-kpc scale (typical size scale of high- z GMCs), which enables us to compare the spatial distributions of star-forming gas clumps with recent star-formation (from HST). Such comparisons are the key to understand different processes that regulate the star-formation/SB in ULIRGs/mergers and examine how they differ from other galaxy populations. We will also measure the linewidths of the very dense gas (traced by HCN and HCO $^+$), the excited gas (traced by CO($J=5 \rightarrow 4$)), and the more-extended, less-perturbed molecular gas (traced by low- J CO) at various regions within the AGN host galaxy to constrain the kinematics and relative mass-fractions of different gas phases, which are

indications of the evolutionary stage of a galaxy.

Line ratios and the AGN/SB diagnostic: Aided by lensing, we will be able to obtain kinematical information on spatial scales smaller than the beam, as seen in our CO($J=2 \rightarrow 1$) data (Fig. 4c, d), thereby enabling us to probe the physical properties of the inner molecular disk near the AGN. Recent studies find that the HCN($J=4 \rightarrow 3$)/HCO⁺($J=4 \rightarrow 3$) line ratio is expected to be enhanced in the circumnuclear disk (CND) near an AGN and falls off with distance from the CND (García-Burillo et al. 2014; Imanishi et al. 2016). At the proposed resolution, we will resolve the line emission originating near the AGN and that from the spatially extended SB regions (>kpc scale) in the host galaxy, and by measuring spatial variations in this line ratio, we will assess its utility as an AGN/SB diagnostic (Fig. 2) at high redshift. Since the HCN vibrational line ($v_2=1$) falls within the targeted frequency range, we will use it to independently constrain the radiation properties of the AGN environment, given that this line is excited by infrared pumping and that the radiation field associated with the AGN is the cause of the elevated HCN($J=4 \rightarrow 3$)/HCO⁺($J=4 \rightarrow 3$) (Sakamoto et al. 2010; Imanishi & Nakanishi 2013). The proposed spatial resolution is also necessary for a detailed lens modeling of each emission line, enabling measurements of reliable line ratios, without significant uncertainties due to differential lensing. Such measurements are vital to reveal how galaxy interactions drive gas into inner disks to initiate SB/AGN activities and how the ISM differ from normal star-forming galaxies.

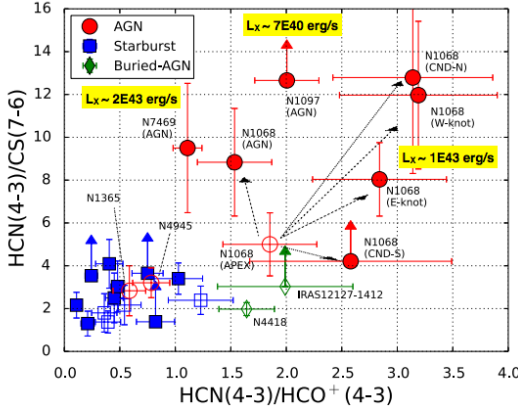


Figure 2: HCN($J=4 \rightarrow 3$)/HCO⁺($J=4 \rightarrow 3$) as AGN/SB diagnostic Difference in line ratios between local AGNs, SBs, and (U)LIRGs with buried AGNs suggest that HCN($J=4 \rightarrow 3$)/HCO⁺($J=4 \rightarrow 3$) can be used as a diagnostic tool to reveal the dominant power source within the beam, where an elevated line ratio is seen in AGN and circumnuclear regions relative to SB regions/galaxies. Such diagnostic depends heavily on the spatial resolution, as demonstrated by the measurements taken with APEX (empty circle) and ALMA (filled circles) in NGC1068. We here propose to spatially resolve this line ratio within the AGN host galaxy and obtain measurements near the AGN and the extended SB regions to investigate spatial variations in order to assess its utility as a AGN/SB diagnostic at high redshift. (Figure taken from Izumi et al. 2016)

Since CO($J=5 \rightarrow 4$) is excited in higher temperature than the HCN and HCO⁺ lines (e.g. in X-ray dominated regions (XDRs) near an AGN), variations in HCN/CO will allow us to constrain the spatial extent of photon-dominated regions (PDRs from SBs) and XDRs. In addition, we will measure spatially resolved line ratios of HCN/CO and HCO⁺/CO within the AGN host galaxy as proxies of its very dense (cores; $\sim 10^5$ - 10^7 cm⁻³) versus the less dense (clumps; $\sim 10^4$ cm⁻³) gas content and their spatial distributions as a function of distance from the AGN/nucleus. This will enable us to gain insight into the interplay between AGN, SB and the dense gas content in the ISM (and thus the SF mode on small scale across different galaxy populations as traced by the HCN/CO- L_{IR} relation). We will also combine CO($J=5 \rightarrow 4$) with our existing CO($J=2 \rightarrow 1$) and CO($J=3 \rightarrow 2$) data to constrain the gas density (n_{H_2}) and kinetic temperature by performing large velocity gradient modeling.

The SK Law for dense gas: The Schmidt-Kennicutt (SK) relation ($\Sigma_{\text{SFR}} \propto \Sigma_{\text{gas}}^N$; Fig. 3) is one of the key ingredients for theoretical models as it encodes the physical processes and timescales regulating star-formation and their dependence on the ISM (e.g. Narayanan & Krumholz 2014). However, the surface density of gas at high densities ($n_{\text{crit}} \gtrsim 10^5$ cm⁻³; Σ_{dense}) is currently poorly constrained for high- z galaxies due to the lack of (spatially resolved) observations of the much weaker emission from high critical density tracers. It is thus unclear how the power-law index of the SK law should change depending on the critical density of the tracer used to probe the SF gas (e.g. Krumholz & Thompson 2007) and how the SFR surface density should depend on the global dynamical time scales in normal galaxies and in mergers. At the proposed resolution, we will spatially resolve, for the first time, the *true SK relation* by measuring the dense gas surface density ($n_{\text{crit}} \gtrsim 10^5$ cm⁻³) in a high- z merger, down to the size scale of star-forming gas clumps. This will enable us to provide crucial constraints on star-formation at high redshift.

Our proposed observations therefore provide an exceptional opportunity to investigate the physical prop-

erties and dynamical structures of different gas phases in the ISM of mergers and distant galaxies with exquisite details. Such investigations are vital to bridge the gap in our current understanding on different galaxy populations across cosmic time. This will also demonstrate the capabilities of ALMA in utilizing these much fainter high-dipole moment molecules as routine tracers to study star-formation at earlier epochs.

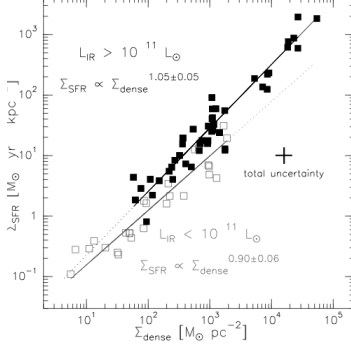


Figure 3: Schmidt-Kennicutt relation for dense gas While constraints on the power-law index from gas of different densities are important for star-formation models, current studies only have constraints up to the gas of density traced by the ground state HCN line ($n_{\text{crit}} \sim 10^4$), which are also largely limited to local measurements (García-Burillo et al. 2012). Our proposed observations will, for the first time, spatially resolve the SK relation at kpc scale in a ULIRG at $z \sim 0.7$ by using high critical density tracers (HCN($J=4 \rightarrow 3$) and HCO⁺($J=4 \rightarrow 3$)). This will allow us to explore potential deviations at higher redshift and provide key constraints for models of galaxy evolution.

Technical overview We estimate the source size from our lens model and adopt conservative line ratios measured for ULIRGs and high- z galaxies (GS04; P07; Greve et al. 2009; Carilli & Walter 2013) to compute the estimate line fluxes. To secure enough S/N for lens modeling, we require a minimum of 8σ of $0.47 \text{ mJy beam}^{-1}$ and $0.07 \text{ mJy beam}^{-1}$ per 150 km s^{-1} channel for the science goals, respectively (see TJ for details).

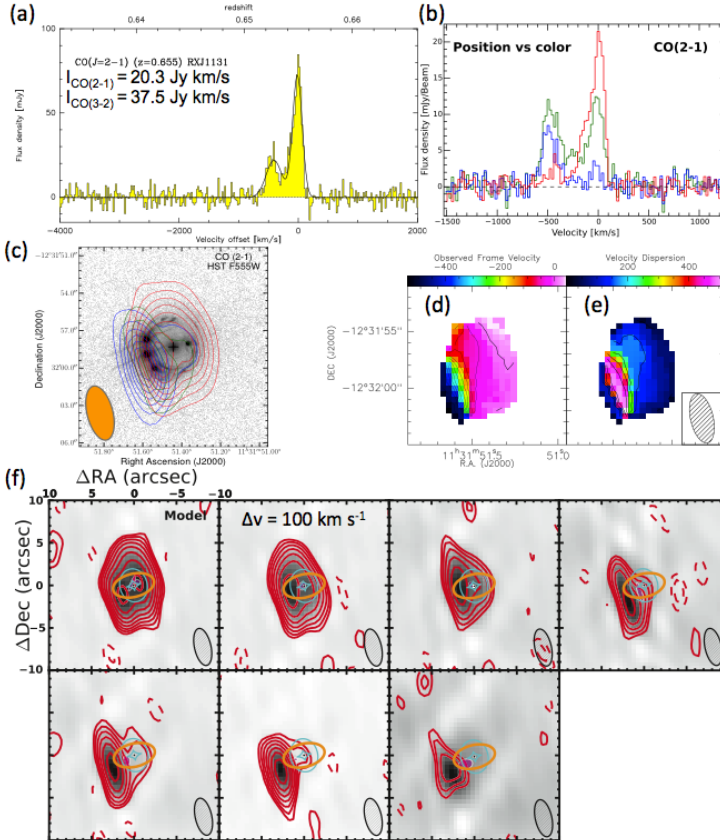


Figure 4: CO($J=2 \rightarrow 1$) (a): A double-horned line profile from the AGN host galaxy, which appears asymmetric due to differential lensing. (b): Spectra taken at three locations along the strongest velocity gradient, demonstrating differential lensing of the kinematic components of the gas-rich “disk”. (c): Observed spatial variations across the channels, as shown by the red (red-shifted), green (line center), and blue (blue-shifted) contours. (d, e): The observed velocity gradient and velocity dispersion are suggestive of a kinematically ordered disk at the current resolution limit. The spectrally resolved lensed emission allows us to probe dynamical structures on smaller spatial scales than otherwise possible. (f): Channel maps of the CO emission (red) overlaid on our best-fit lens models (grayscale). The foreground lensing galaxy is represented by a black dot. The reconstructed source morphology (magenta ellipses) is also suggestive of a “disk”. Given the presence of a companion galaxy within 2.4 kpc and beam smearing effects, high-resolution imaging is necessary to unambiguously determine the structure that gives rise to the observed velocity gradient and dispersion, as proposed here. This will allow us to investigate the mechanisms responsible for the starburst in the AGN host galaxy and its ISM conditions as it interacts with the companion. We therefore aim to spatially resolve the gas dynamics, kinematics and ISM conditions in a merger, providing observational constraints on the star-formation processes at an epoch where the SFR density is steeply rising across cosmic times.

References • Brewer et al. 2008, MNRAS, 390, 39 • Carilli et al. 2013, ARA&A, 51, 105 • Claeskens et al. 2006, A&A, 451, 865 • Gao et al. 2007, ApJ, 660, L93 • Gao et al. 2004, ApJ, 606, 271 • García-Burillo et al. 2014, A&A, 567, A125 • García-Burillo et al. 2012, A&A, 539, A8 • Greve et al. 2009, ApJ, 692, 1432 • Imanishi et al. 2013, AJ, 146, 91 • Imanishi et al. 2014, AJ, 148, 9 • Imanishi et al. 2016, ArXiv e-prints • Izumi et al. 2016, ApJ, 818, 42 • Juneau et al. 2009, ApJ, 707, 1217 • Krumholz et al. 2005, ApJ, 630, 250 • Krumholz et al. 2007, ApJ, 669, 289 • Narayanan et al. 2014, MNRAS, 442, 1411 • Papadopoulos, P. P. 2007, ApJ, 656, 792 • Rangwala et al. 2015, ApJ, 806, 17 • Riechers et al. 2007, ApJ, 671, L13 • Riechers et al. 2010, ApJ, 725, 1032 • Sakamoto et al. 2010, ApJ, 725, L228 • Shirley et al. 2003, ApJS, 149, 375 • Sluse et al. 2003, A&A, 406, L43 • Swinbank et al. 2012a, ApJ, 760, 130 • Swinbank et al. 2012b, MNRAS, 426, 935 • Viti et al. 2014, A&A, 570, A28 • Wagg et al. 2005, ApJ, 634, L13 • Wu et al. 2005, ApJ, 635, L173 • Zhang et al. 2014, ApJ, 784, L31